MDPI

Advanced Road Safety: Collective Perception for Probability of Collision Estimation of Connected Vehicles

Sabrine Belmekki [1,*] and Dominique Gruyer [2]

1 LEOST Laboratory, COSYS, Gustave Eiffel University, Villeneuve d'Ascq, 59650 Lille, France
2 PICS-L Laboratory, University Gustave Eiffel, 25 allée des Marronniers, 78000 Versailles, France
* Correspondence: sabrine.belmekki@univ-eiffel.fr

Abstract: In the dynamic landscape of vehicular communication systems, connected vehicles (CVs) present unprecedented capabilities in perception, cooperation, and, notably, probability of collision management. This paper's main concern is the collision probability of collision estimation. Achieving effective collision estimation heavily relies on the sensor perception of obstacles and a critical collision probability prediction system. This paper is dedicated to refining the estimation of collision probability through the intentional integration of CV communications, with a specific focus on the collective perception of connected vehicles. The primary objective is to enhance the understanding of the potential probability of collisions in the surrounding environment by harnessing the collective insights gathered through inter-vehicular communication and collaboration. This improvement enables a superior anticipation capacity for both the driving system and the human driver, thereby enhancing road safety. Furthermore, the incorporation of extended perception strategies holds the potential for more accurate collision probability estimation, providing the driving system or human driver with increased time to react and make informed decisions, further fortifying road safety measures. The results underscore a significant enhancement in collision probability awareness, as connected vehicles collectively contribute to a more comprehensive collision probability landscape. Consequently, this heightened collective collision probability perception improves the anticipation capacity of both the driving system and the human driver, contributing to an elevated level of road safety. For future work, the exploration of our extended perception techniques to achieve real-time probability of collision estimation is proposed. Such endeavors aim to drive the development of robust and anticipatory autonomous driving systems that truly harness the benefits of connected vehicle technologies.

Keywords: connected vehicles; collective perception; collision probability of collision estimation; integrated communication strategies; road safety enhancement

1. Introduction

In recent years, vehicular communication has evolved, driven by the rapid convergence of emerging technologies. Among the most promising advancements in this domain is the emergence of Connected Vehicles (CVs), a paradigm that has revolutionized traditional concepts of mobility, safety, and efficiency.

This system comprises various vehicular components, including radar detectors, forming a joint automotive radar and vehicular communication system that utilizes the dedicated automotive bandwidth for both applications, as explained by Wang et al. and Aydogan et al. [1,2]. The distinctive characteristics of vehicular ad hoc networks (VANETs), characterized by high mobility, frequent topology changes, sporadic connectivity, and limited communication range, present intricate challenges in designing effective routing protocols as explained in the work of Sharma and Nidhi [3]. The central goal of VANET routing protocols is to establish reliable and efficient communication pathways between vehicles, infrastructure nodes, and even pedestrians. Achieving this objective necessitates a

delicate equilibrium between optimizing communication performance and adapting to the dynamic nature of vehicular networks.

Researchers in the VANET domain have delved into designing routing strategies that tackle diverse challenges [4,5].

Safety-critical applications, such as collision avoidance and emergency messaging, demand ultra-low latency and high reliability [6]. To cater to these demands, protocols like geographic routing and beacon-less routing focus on swift message dissemination while considering vehicular movement patterns. In contrast, traffic efficiency applications, such as traffic congestion mitigation and route planning, require strategies, ensuring efficient data dissemination and load balancing. Protocols like probabilistic broadcasting and cluster-based routing leverage the collaborative nature of vehicular networks to effectively distribute traffic-related information. Various studies have established a classification of existing clustering approaches [7–10]. This approach, as outlined, enhances the effectiveness of routing protocols by reducing control traffic and simplifying data routing [11–13]. Several clustering algorithms have been proposed and evaluated by Cooper et al. [10]. Notably, Husnain et al. [14] introduced a probabilistic clustering method inspired by whale behavior in VANETs, employing the p-WOA algorithm.

Central to this transformation is the concept of collective perception; this is an innovative approach that harnesses the collaborative capabilities of interconnected vehicles to enhance sensor perception, information exchange, and probability of collision management. Collective perception exploits vehicular networks to create a comprehensive and dynamic understanding of the environment, as depicted in the work of Shan Mao et al. [15]. Through seamless real-time data exchange, networked vehicles access an extended sensory range, surpassing the limitations of individual sensors, including radars. This framework enables vehicles to collectively "see" and "sense" beyond their immediate line of sight, establishing a virtual sensor network that spans the entire vehicular ecosystem.

The advent of collective perception holds wide-ranging implications across road safety, traffic management, and autonomous driving. By amalgamating sensor data and insights, collective perception enhances obstacle detection accuracy, road condition assessment, and hazard anticipation. Consequently, this fosters a safer driving environment, enabling intelligent transportation systems to make informed real-time decisions. Notably, connected vehicles enhance traffic safety in foggy conditions, with results indicating significant improvements through CV approaches [15–17]. Research has demonstrated that utilizing cooperative automated vehicles (CAV) can reduce the frequency of rear-end conflicts at signalized intersections by 40% (according to Fyfe et al. [18]), improve the safety index by up to 45% (according to Olia et al. [19]), and demonstrate improved safety and mobility on highways in the context of CV [20].

Rahman, M.S. et al. and Karbasi et al. [16,21] have demonstrated that connected vehicles can improve traffic safety in foggy conditions, with the results indicating that both CV approaches significantly improve safety. AVs may not accurately identify environmental factors with 100% certainty, such as road boundaries, lanes, rules, and signals. AVs possess a certain level of confidence or degree of certainty about these aspects, as described by Freitas et al. [22]. The use of deep learning sensor fusion algorithms has shown potential to improve the performance of AV systems in short-range or local vehicle environments, with a focus on perception, localization, and mapping [23].

In [24], Tian et al. proposed a stochastic model to evaluate the collision probability for a heterogeneous vehicle platoon, which accounted for the distribution of inter-vehicle distances. However, the model did not consider other factors that may contribute to collisions, such as road geometry, vehicle speed, and driver behavior. Despite its limitations, the model has the potential to provide valuable insights into the potential reduction of chain collisions and their severity.

The adaptation of the CBL-G system to support the collective perception message (CPM) and the inclusion of better indicators for the probability of collision estimation can

result in significant benefits. However, the use of CPMs may increase the probability of collision of saturating the communication channel and making the network unstable.

The purpose of this paper is to refine the collision probability of collision estimation in intelligent transportation systems, particularly focusing on connected vehicles (CV). By integrating CV communications and emphasizing collective perception, this paper aims to enhance the understanding of the potential collision probability of collisions. Through extended perception strategies, the goal is to provide improved anticipation capabilities for both the driving system and human drivers, thereby contributing to heightened road safety. The study's results underscore a significant enhancement in collision probability awareness, emphasizing the potential for more robust and anticipatory autonomous driving systems.

This paper is described as follows: We analyze existing methods of collective perception for collision probability estimation of connected vehicles (Section 2). The study introduces a new collective perception level (Section 2.1), including extended local perception (Section 2.1.1), extended branch perception (Section 2.1.2), and global perception (Section 2.1.3).

We further investigate existing methods for estimating the probability of car collisions, focusing on vehicle modeling with uncertainties and multi-dimensional configuration modeling between vehicles (Section 3). We describe the simulation configuration in Section 4.

Proposing a multi-level approach, we present the local probability of collision estimation, extended local probability of collision estimation, extended branch probability of collision estimation, and global probability of collision estimation (Section 5). The paper concludes with insights and future perspectives on collision probability of collision estimation for intelligent transportation systems (Section 6).

1.1. Communication Strategy

For our study, the communication and environment system is described as follows: To start, we used the algorithm of Sabrine Belmekki et al. [25,26]. It is a decentralized approach known as CBL-G (chain branch leaf gateway). It operates on the principle of establishing a hierarchical structure among communication nodes to form clusters. This allows each "cluster member" node to communicate directly with a "cluster head" node through a single hop, without the need to rely on an intermediate node. It uses additional infrastructure nodes (roadside unit-RSU) as a gateway to enhance the coverage (QoS) quality of service [27].

CBL architecture features a centralized design for each cluster, where only the branch node can establish communication with other clusters. In this way, CBL distinguishes two distinct node types: "branch" nodes and "leaf" nodes. Both types of nodes broadcast periodic HELLO messages to dynamically construct a structure known as a "chain." The chain connects the "branch" nodes and, by extension, the clusters in each direction, as illustrated in Figure 1.
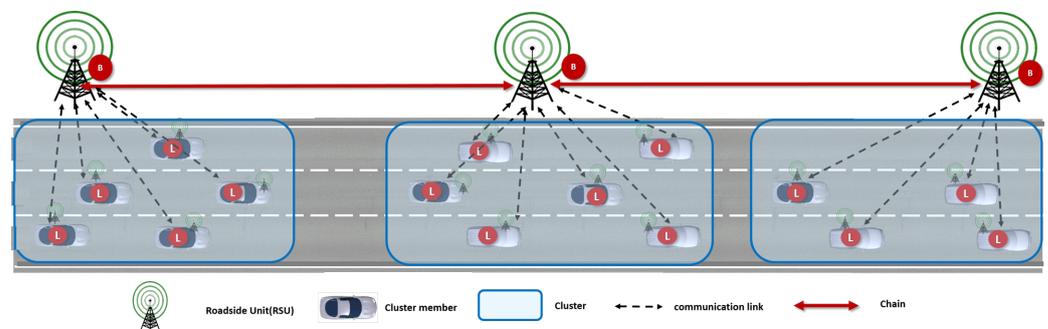

Figure 1. The CBL-G infrastructure representation of vehicles on a three-lane highway and full deployment of roadside units.

CBL employs a metric—known as the connection time—to construct stable chains. This metric measures the time it takes for nodes in the network to connect and allows nodes

to manage the selection of their branch node. The following are the definitions of "branch" nodes, "leaf" nodes, chain, and connection time:

The branch: The "branch" node is the cluster head elected by other nodes within its 1-hop neighborhood. It sends HELLO messages like other nodes but has exclusive permission to send topology control messages, transmit request messages, and participate in chain construction. A "branch" node can relay messages to its leaf nodes, upstream and downstream branches, and branches in other directions of traffic, based on the request specified in the header fields.

The leaf: A leaf node is a regular node that connects to the nearest branch node. When no branch node is detected, the leaf node chooses the neighbor moving with the lowest speed and in the same direction as its branch. A leaf node only sends HELLO messages and application data traffic.

The chain: The resulting CBL structure is comparable to a virtual spinal structure that is maintained through links between the nodes. Each node contains the following parameters: BranchChoice (the address of a selected branch node), ChainUP (the address of the branch node to relay upstream traffic), ChainDO (the address of the branch node to relay downstream traffic), and connection time (CT), which is the expected communication duration between two nodes that maintain the same speed. BranchChoice is null if the node is a branch, and ChainUP/ChainDO are empty if the node is a leaf.

1.2. Cbl-G Functional Diagram

The diagram represented in Figure 2 unwinds the mechanism of CBL-G from the reception of a Hello message until the end.
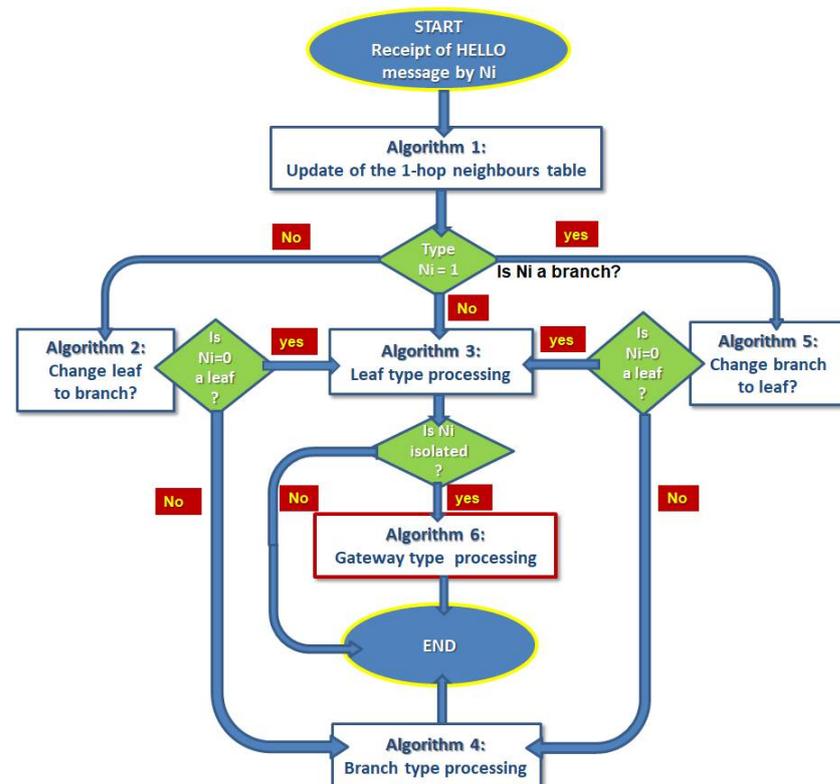

Figure 2. CBL-G algorithm processing upon reception of a Hello message.

A leaf node endeavors to establish a connection with a branch node located a single hop away from its current position. This process of neighborhood discovery occurs through the periodic transmission of the "HELLO" message, persisting even after integration into a cluster.

In cases of isolation, where neighboring nodes remain undetected, the leaf node designates the roadside unit (RSU) as its proximate branch node. The arrival of a branch node within its range triggers the identification of a potential branch in the vicinity. This prompts the branch node to disengage from the RSU and form a connection with the newly identified branch.

The RSU assumes the role of a relay point for isolated vehicles, facilitating their connection to the infrastructure. Simultaneously, the isolated node identifies a branch for affiliation, effectively averting its isolation. Post-integration with the RSU, the previously isolated leaf nodes persist in periodic "HELLO" message-based neighborhood exploration.

Upon detecting a neighboring node, an isolated leaf node follows the connection protocol akin to the chain branch leaf (CBL) approach. Should the offered connection time (CT) surpass that provided by the RSU, the leaf node nominates the detected node as its connecting branch.

Subsequently, the elected branch node endeavors to find another branch for chain formation. In cases where such a branch is not found, a leaf node is designated as the front branch. Subsequent nodes along the route identify the presence of branches and establish connections accordingly.

2. Analysis of Existing Methods of Collective Perception for Collision Probability Estimation of Connected Vehicles

In the context of V2X communications, the CPM generation rules dictate the frequency and content of CPM transmissions. The ETSI standard establishes that a vehicle must check every CPM generation time (T_GenCpm) interval to determine if a new CPM should be generated and transmitted, with T_GenCpm ranging between 0.1 s and 1 s [28].

A new CPM must be generated if a new object is detected or if certain criteria, such as position or velocity changes, are met for previously detected objects. The frequency of CPM transmissions and the amount of information included in each message can impact the overall channel load and reliability of V2X communications.

In CBL-G, a periodic control message, referred to as the "HELLO message", is used to discover neighboring vehicles. The HELLO message and the CPMs are important to distinguish, as the first maintains the communication architecture and link between vehicles, while the second, the CPM, shares each vehicle's perception information, allowing for the expansion of the nodes's local map.

The vehicle is assumed to have a frontal view of 200 m and a communication range of 500 m. The ego vehicle generates CPMs following ETSI's current CPM generation rules (Figure 3). Upon receiving a new control message from a neighboring vehicle V_j, vehicle V_i will send a CPM containing information about the detected object V_j. If vehicle V_i does not detect any new vehicle after one second, it will send an empty CPM message, to signal that it can detect and share objects.

The adaptation of CBL-G for the collective perception is conducted by the adaptation of the structure of the vehicle; indeed, we introduce a new element, which is the detected object.

Vehicle Vi			Vehicle Vj										Date
Identifier	Position	Speed	Identifier	occurrence	Position	Speed	Node's Type	Acceleration	heading	Dimensions	Mass	Confidence	Time of measurement
ID	X Y	V1 V2	ID	Occ	X Y	V1 V2	Type	A	Heading	Length Width	M	C	Date

Figure 3. Our collective perception message proposition.

To address these findings, we considered incorporating specific parameters into the structure of our vehicle to accommodate various usage scenarios. Consequently, we

integrated several additional fields, such as acceleration, dimensions (length × width), mass, trajectory, occurrence, and vehicle type (urban, van, motorcycle, etc.).

These new parameters are necessary to improve the accuracy of the perception system by enabling more precise identification and tracking of vehicles within the environment. By considering these factors, we can develop more robust and effective perception systems that can operate in a variety of environments and under different conditions.

2.1. Collective Perception Level Proposal

Autonomous vehicles rely on perception systems to make decisions and ensure safety while navigating through different scenarios. The perception system's performance heavily depends on the density of the environment and the number of leaves per branch. CBL-G is an architecture that can be used to enhance the perception of autonomous vehicles.

The local perception is limited to the capacity of the onboard sensor i.e., it is limited to its perceptive capacity and the surrounding obstacles (fields of vision). Figure 4 represents the local perception of vehicle F1, which is vehicle F2.
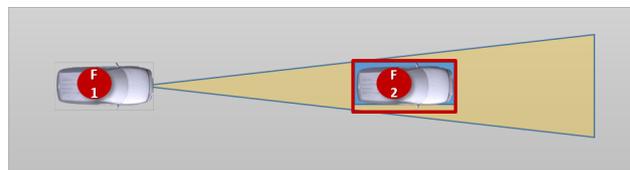

Figure 4. Vehicle "F1" local perception representation.

In this study, we measured the number of leaves per branch and the local probability of collisions calculated per branch for different scenarios using the CBL-G architecture. We found that the number of leaves per branch in CBL-G is about 1.94 for low-density scenarios (S1), 4.75 for medium-density (S2), and 7.03 for high-density (S3). However, due to the perception limitation, the mean number of obstacles perceived per branch is 0.5 in a low-density scenario (S1), 3.48 in a medium-density scenario (S2), and 5.89 in a high-density scenario (S3). This results in a loss of important data. We propose establishing different levels of extended perception for connected vehicles in the CBL-G structure.

2.1.1. The Extended Local Perception

The extended local perception is a mechanism that enables a cluster head to obtain a shared perception of its cluster members, thereby allowing it to perceive the actions of its leaves. In the context of vehicular networks, the extended local perception approach is employed to enhance a branch's perception by using information shared by its leaves.

As depicted in Figure 5, the local perception of vehicle B does not provide information about the presence of any vehicles. However, utilizing the information perceived by vehicles L1 and L3, we can detect the presence of vehicles L2 and L4.

This example demonstrates how the extended local perception approach can be applied to limit the perception to the front zone of vehicles (i.e., RADAR) and model the uncertainties on vehicle localization obtained with GPS, as well as frontal obstacle detection obtained with RADAR.

Thanks to the CBL communication system, a branch can receive the local perceptions of its leaves (L1, L2, L3, L4). Consequently, while the perception of B may be empty, its extended local perception will contain the four nodes of its cluster (L1, L2, L3, L4), as illustrated in Figure 5. The extended local perception approach allows a branch to detect more vehicles, on average, than those directly connected to the branch since it utilizes information shared by the leaves to enhance the branch's perception.

The average number of new nodes perceived by a branch using the extended local perception approach was calculated to be 1 new node in low-density environments, 6.96 new nodes in medium-density environments, and 11.78 new nodes in high-density

environments. However, the accuracy of the perception heavily relies on several factors, such as traffic density, perception distance, and the quality of perception sensors utilized.
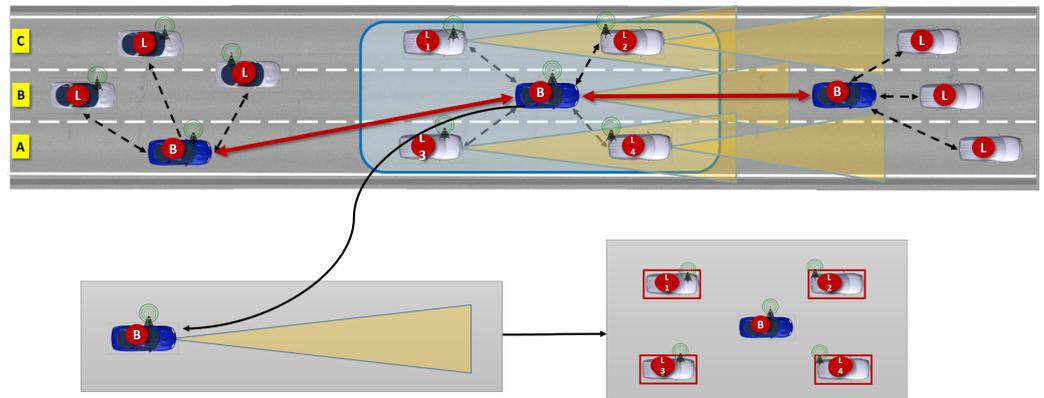

Figure 5. Vehicle "B"; the extended local perception representation.

2.1.2. The Extended Branch Perception

The extended branch perception involves the perception of the downstream neighboring branch shared with its upstream branch and the perception of the upstream neighboring branch shared with its downstream branch. This allows the central branch to receive perceptions of objects (obstacles) that it cannot see using only its embedded equipment from both sides (upstream and downstream). We can perceive further than we could previously with extended local perception, which is limited to the cluster.

Figure 6 illustrates the extended branch perception case: The extended branch perception of vehicle B2 does not allow it to detect any vehicles. However, thanks to the CBL communication system, the branch will receive the local perceptions of its upstream and downstream branches (B3, B1).

Indeed, as the adjacent branches communicate to form a chain, the B2 branch will also be able to receive the GPS positions of the B1 and B3 branches. The collection of all the information on the branch's perception will then make it possible to estimate a map of the extended branch perception, which can be used to build a map of the extended branch probability of collisions. B1 will share its perception with its upstream branch, Branch B2.
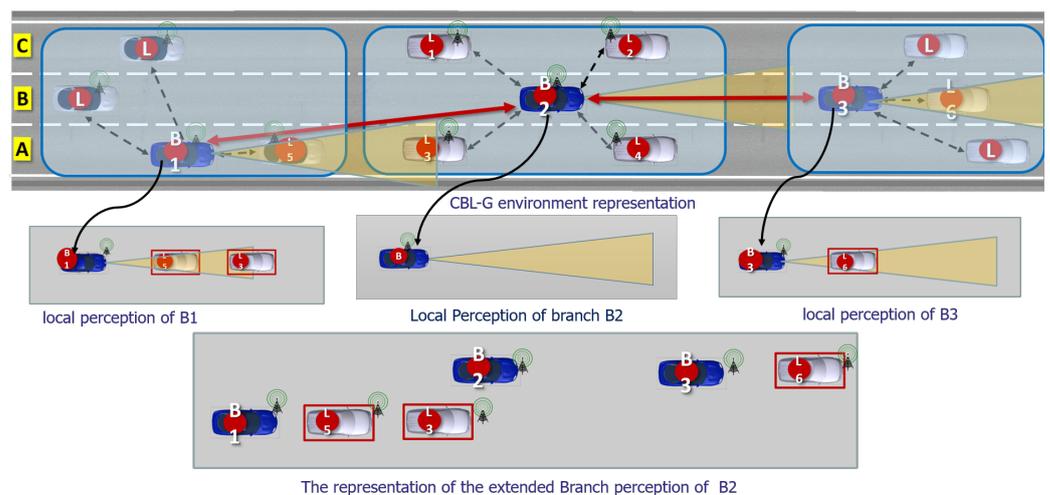

Figure 6. Representation of Branch B2's extended perception in the CBL environment.

B3 will share its perception with its downstream branch, Branch B2. Node B2 possesses a perception that solely comprises its own location information. Meanwhile, Node B1 generates a dynamic perception, incorporating its location and the detection of Nodes

L5 and L3. Similarly, Node B3 generates a similar map, comprising its location and the detection of Node L6.

From these perceptions, Branch B2 builds its own extended branch perception. Utilizing the extended branch perception approach, which involves the local extended perception of neighboring branches, we determined the average number of new nodes perceived by a branch to be 0.56 new nodes in low-density environments, 3.05 new nodes in medium-density environments, and 5.69 new nodes in high-density environments. However, since some vehicles can be detected both in the extended local perception of neighboring branches and in the extended local perception of leaves connected to a branch, using the extended local perception of neighboring branches may result in the redundant detection of nodes that have already been perceived in the extended local perception of leaves connected to the central branch.

Nonetheless, there are instances where the extended local perception of leaves connected to a branch does not cover all nodes in a densely populated area around the central branch, leading to gaps in detection. In these cases, utilizing the extended local perception of neighboring branches can cover a wider area and detect nodes that were not perceived in the extended local perception of the leaves connected to the central branch.

2.1.3. The Global Perception

Expanding the perception of the ego vehicle beyond its immediate vicinity is achieved by utilizing the perception of branch nodes positioned further than the upstream and downstream nodes of its location. This technique, known as global perception, facilitates the sharing of perception information among more distant branch nodes.

This approach provides the ego vehicle with a comprehensive understanding of its surroundings, including areas that are beyond the immediate upstream and downstream clusters, thus enabling the projection of global situational awareness while the vehicle is in motion.

By employing the global perception approach, which extends local perception to distant neighboring branches, we observed that the number of new nodes detected varied with the density of the scenario. In a low-density scenario (S1), the average number of newly detected nodes is one. In a medium-density scenario (S2), 3.48 new nodes were detected, and in a high-density scenario (S3), 8.68 new nodes were detected. These findings illustrate that global perception detects a significantly higher number of new nodes compared to local perception extended only to neighboring branches, as shown in Figure 7. This is due to the fact that global perception utilizes more distant branches to augment the central branch's perception, thereby encompassing a wider area and obtaining a more comprehensive view of the environment.
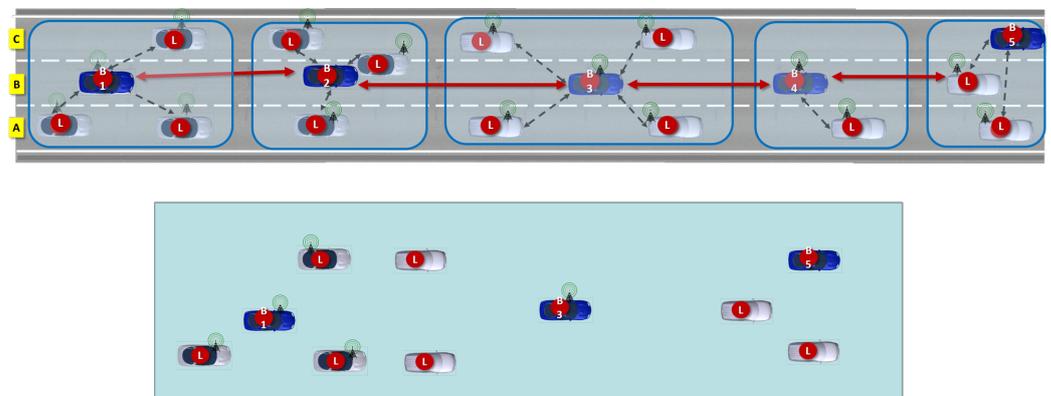

Figure 7. Global perception of B3.

It is important to note that the accuracy of the perception heavily relies on several factors, such as traffic density, perception distance, and the quality of perception sensors utilized. However, the global perception approach provides a more holistic and detailed

understanding of the environment, which is essential for ensuring the safe operation of autonomous vehicles.

The introduction of extended perception levels within the connected-vehicle collision-avoidance system (CBL-G) framework represents a notable advancement in overcoming existing limitations. By incorporating local, branch, and global perception approaches, this proposal aims to comprehensively evaluate the probability of collision in connected vehicle scenarios. Each perception level brings forth distinct advantages and challenges, contributing to a nuanced understanding of collision probability of collision dynamics.

The exploration of local perception allows for a detailed assessment of immediate surroundings, providing the system with granular data for potential collisions in close proximity. However, it may be limited in anticipating collisions beyond its immediate vicinity.

Branch perception, on the other hand, extends the system's awareness along specific trajectories or pathways, enabling a more proactive approach to potential collision probability of collisions. This approach introduces challenges related to accurately predicting the future behavior of surrounding entities.

Global perception, encompassing a broader spatial context, offers a comprehensive view of the environment, allowing for a more holistic evaluation of the collision probability of collisions across varied scenarios. Nevertheless, this approach may present challenges in terms of real-time processing and the potential for information overload.

By systematically exploring these extended perception levels, the CBL-G structure seeks to strike a balance between granularity and scope, aiming to enhance the system's ability to evaluate the collision probability of collision in diverse connected vehicle environments. This multifaceted approach holds promise for advancing the collision probability of collision assessment, contributing to the overall safety and effectiveness of connected vehicle communication systems.

3. Analysis of Existing Methods for Estimating the Probability of Vehicle Collisions

In recent years, there has been a significant increase in research efforts toward collision probability of collision estimation methods between autonomous and connected vehicles. This is driven by the need for safe and efficient transportation in future intelligent transportation systems.

The time-to-collision (TTC) metric combines spatial proximity and speed to estimate the probability of collision; it is considered reliable but ineffective in low congestion periods and for measuring lane change conflicts [29,30]. Extended perception and alternatives such as modified time to collision (MTTC) evaluate collision likelihood over time, while TTC provides a snapshot of the situation at a specific point in time. Time-integrated time-to-collision (TIT) is used to evaluate the collision-avoidance system performance but only under congested highway conditions.

According to Charly et al. [30], during low congestion periods, such as overnight, the use of TTC alone is insufficient. While TTC can be used directly from the perspective of the following vehicle in simple two-vehicle scenarios, Demmel et al. [31] state that extended perception can enable more complex representations of driving collision probability. However, due to the limitations of TTC in complex scenes, alternative approaches such as time-to-closest-encounter (TTCE) have been proposed. Eggert et al. [32] describe TTCE as an improved version of TTC, which accounts for occlusion and dynamic objects, and utilizes a Gaussian and spatial occupancy probability approach as well as survival analysis.

Modified time-to-collision (MTTC) provides a comprehensive view of the likelihood of a collision over time, considering various scenarios and conditions. It is often used to evaluate the performance of collision-avoidance systems. On the other hand, TTC, or time-to-collision, measures the time elapsed between the detection of a potential collision and the actual impact, providing a snapshot of the situation at a specific point in time. While both are used to evaluate the probability of collision of a collision, TTC focuses on the immediacy of a potential collision, while MTTC considers the average time it takes for a collision to occur, taking various factors into account.

TIT, or time-to-impact, is another measure used to evaluate the performance of collision-avoidance systems. It measures the time elapsed between the detection of a potential collision and the actual impact, similar to TTC [33]. However, TIT is considered more effective at capturing individual crash probability of collision, especially under congested highway conditions [33]. Integrating important aspects of different driving environments into an indicator, such as connecting lanes or ramps, can also provide insights into collision probability of collision [34,35].

Responsibility-sensitive safety (RSS) is a mathematical formulation of the duty of care in autonomous vehicle safety [36]. It takes into account various factors, including reaction time and maximum acceleration, to determine a vehicle's ability to avoid a collision. One of the key advantages of RSS is its consideration of additional factors, such as the state of the ego-vehicle, road geometry, and environmental parameters, making it a more complete indicator in terms of key elements present in a driving scenario [37,38]. However, the implementation of the RSS indicator may have limitations, such as the requirement for precise data input and the potential added complexity to the driving experience.

A game-theoretic approach was proposed by Fox et al. [39] to estimate the collision probability of collisions of two autonomous vehicles in a merging scenario. However, game theory models can be computationally expensive to solve, which can limit their real-time applications Muzahid et al. [40] provided an AI-enabled conceptual framework and a decision-making model with a concrete structure of the training network settings.

This paper's main concern is the collision probability of collision estimation, as highlighted in previous sections; achieving effective collision estimation heavily relies on the sensor perception of obstacles and a critical probability of collision prediction system. Improving these details will require extensive research and development to enable real-time perception and tracking of more objects, as discussed in Section 2.1.

Additionally, Section 3 discusses various proposed metrics for estimating the driving probability of collision based on parameters such as speed, time, or distance between vehicles. However, these metrics have limitations in accounting for uncertainties and multi-dimensional factors that are essential to represent the complexity of the driving environment.

3.1. Vehicle Modeling with Uncertainties

To model the configurations between two vehicles in the driving environment, it is important to have a physical representation of the two objects. In our methodology, we denote the vehicles as rectangles with five geometrical points: the center of the rectangle and the four angles of the rectangle [41]. The coordinates of these points are determined using the length and width of the vehicle, as shown in Equation (1).

$$x_i = x_e \pm \frac{L}{2}; \qquad y_i = y_e \pm \frac{W}{2} \tag{1}$$

where L and W are the length and width of the vehicle, and x_e and y_e are the coordinates of the center of the rectangle.

To model the position uncertainties due to the accelerations of the moving objects, we assume that the borders of the vehicle shape (space occupancy) are slightly farther away. Therefore, an acceleration value is applied to the current vehicle or obstacle positioning, resulting in extended vehicle space occupancy coordinates (x'_i, y'_i) with uncertainties. The extended vehicle space occupancy coordinates are given by Equations (2)–(4).

$$x'_{i,front} = x_i + \frac{a_{longi,max}}{2}.dt^2 \tag{2}$$

$$x'_{i,rear} = x_i + \frac{a_{longi,min}}{2}.dt^2 \tag{3}$$

$$y'_i = y_i + \frac{a_{lat,max}}{2}.dt^2 \tag{4}$$

where $a_{longi,max}$ and $a_{longi,min}$ are the maximal and minimal longitudinal accelerations, respectively, $a_{lat,max}$ is the maximal lateral acceleration, and dt is the time step. The lateral acceleration is fixed between -0.5 and $+0.5$ m·s^{-2}, as by Mahajan et al. in [42].

Figure 8 shows the vehicle modeling with uncertainties. The uncertainties are used to represent the configurations of the vehicles in space to assess the relative probability of collision between them.
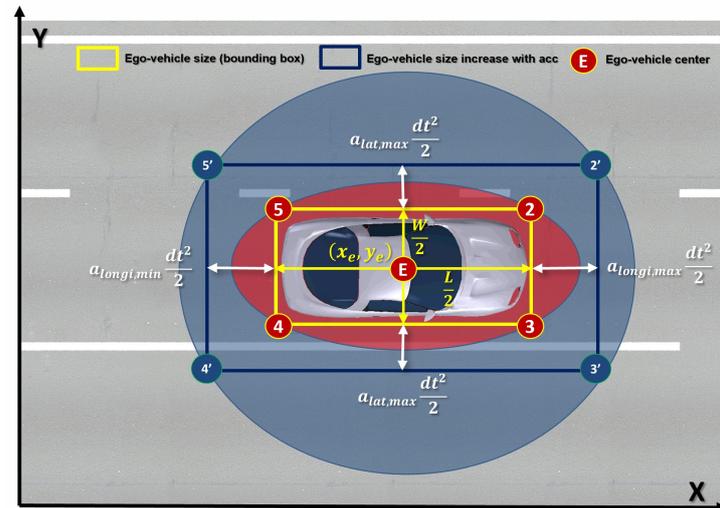

Figure 8. Schematic representation of the vehicle position uncertainties with ellipsoids representing the vehicular space occupancy [41].

3.2. Multi-Dimensional Configuration Model between Vehicles

To take into account the multi-dimensional context with uncertainties, we propose using the Gruyer distance [43] This distance has already been used to assess the distance (similarity) between two vehicles represented by a probabilistic model of a set of points (two clusters of points). The distance function $D_{i,u}$ is defined as follows:

- The function $D_{i,u}$ gives a result scaled between 0 and 1 if the measurement has an intersection with the cluster u. Value 0 indicates that the measurement i is the same object as the cluster u with complete confidence.
- The result is above 1 if the measurement i is out of the cluster u.
- This distance has the properties of distance functions.

4. Experimental Configuration

In our implementation, we utilize two software tools: Firstly, SUMO facilitates the generation of mobility data, and secondly, Matlab (R2020b) is employed to implement the CBL-G architecture.

The scenarios are set on a motorway network modeled as a standard one-way, three-lane highway that spans 5 km in length, with vehicles traveling in the eastbound direction. Each vehicle is assumed to have a randomly generated velocity and is equipped with onboard units (OBUs), enabling communication with others within a range of up to 500 m. Referring to our previous research work [25,26], it is observed that the maximum average frame loss begins to increase after 427 m, with a tolerated frame loss of 26%. The number of roadside units (RSUs) is determined based on the relationship between the optimal number of RSUs and the range of the highway.

Consequently, in the CBL-G simulation environment, each RSU is strategically placed at intervals of 1 km from one another, resulting in a total of 5 RSUs covering the entire 5 km length of the road. This configuration proves sufficient for comprehensive coverage in the simulated scenario.

5. Proposal for Multi-Level Estimates of the Probability of Collision

We introduce a multi-level collision probability of collision estimation method based on CBL-G structure and communication, which aims to estimate the local and extended collision probability of collisions. The CBL-G method will be adapted for CPM and reorganized to include better indicators for the probability of collision estimation.

The goal of calculating the collision probability of collision in the context of the advanced driver assistance system (ADAS) is to enable the definition of various levels of alert, each of which corresponds to a specific reaction. For instance, the lowest level may correspond to audible alerts, while the highest level may involve taking control of the vehicle to avoid an accident. This paper focuses specifically on the estimation of the collision probability, rather than the precise prediction of collision times.

To achieve this goal, a method is proposed that takes into account a set of instants sampled along the predicted interval. The collision probability is then calculated for each sample. This approach allows for the consideration of multiple potential collision events, as opposed to a singular predicted collision time. Additionally, the sampling period is sensor-independent, can be freely adjusted during trajectory prediction, and is finite enough to not interfere with real-time processing.

This paper proposes a method for the multi-level collision probability of collision estimation for connected vehicles (CVs), focusing specifically on the probability of collision estimation rather than the precise prediction of collision times. The proposed approach considers a set of instants sampled along the predicted interval and calculates the collision probability for each sample. This method allows for the consideration of multiple potential collision events, as opposed to a singular predicted collision time. Additionally, the sampling period is sensor-independent and can be freely adjusted during trajectory prediction. It is finite enough to not interfere with real-time processing.

5.1. Local Probability of Collision Estimation

To model the configurations that exist between two vehicles, an ego vehicle, and an obstacle, we studied two different scenarios in different situations.

In selecting vehicle positions and considering speed modes and lane numbers, we prioritized their significant influence on collision probabilities. Our goal was to replicate common and critical scenarios for determining collision probability. The chosen configurations were deemed representative and impactful in the evaluation of the effectiveness of our proposed methodology.

The first scenario (E1) involves the ego vehicle colliding with a slower obstacle vehicle coming from behind on the central lane.

The second scenario (E2) involves the ego vehicle being in lane 2, parallel to the leading obstacle vehicle in lane 3.

5.1.1. Scenario A

To ensure the accurate estimation of the local probability of collision, two scenarios are presented in this study, as shown in Figures 9 and 10. The scenarios are described as follows:

1. Involves the ego vehicle colliding with a slower obstacle vehicle approaching from behind on the central lane (E1).
2. Involves the ego vehicle driving in lane 2, parallel to the lead vehicle (obstacle vehicle) driving in lane 3 (E2).

For scenario E1, the ego vehicle (E) is positioned at 205 m in lane 2 at a speed of 35 m/s. The obstacle leader (vehicle 1) is positioned at 370 m in lane 2, moving at a speed of 15 m/s.

Figure 9. Schematic illustration of scenario 1−E1.

For scenario E2, the ego vehicle (E) is positioned at 431 m in lane 2, traveling at a speed of 20 m/s. The obstacle leader (vehicle 2) is positioned at 491 m in lane 1, also moving at a speed of 20 m/s. Figures 9 and 10 illustrate these scenarios.
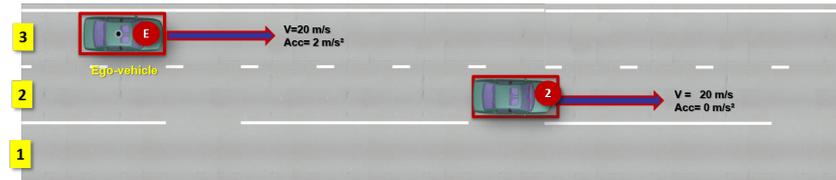

Figure 10. Schematic illustration of scenario 1−E2.

5.1.2. Scenario B: Perception Uncertainty

In this section, we consider scenario B, where we investigate perception uncertainty with perfect vehicle localization using GPS RTK++. Specifically, we assume that the perception of the vehicles is imperfect within their perception field of 200 m. Moreover, the communication within the cluster is perfect, instantaneous, without delay, and without loss.

For scenario 2−E1, as illustrated in Figure 11, the ego vehicle (E) is positioned at 205 m in lane 2, moving at a speed of 35 m·s^{-1}, and the obstacle leader (vehicle 1) is positioned at 370 m in lane 2, moving at a speed of 15 m·s^{-1}.
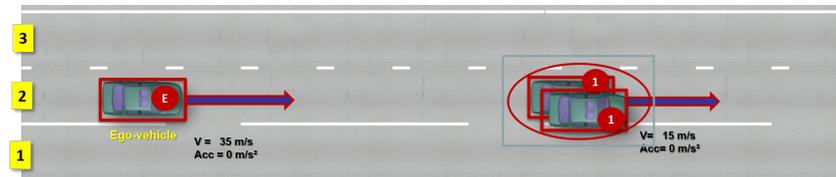

Figure 11. Schematic illustration of scenario 2−E1 with perception uncertainty (scenario B).

Similarly, for Scenario 2−E2, as depicted in Figure 12, the ego vehicle (E) is positioned at 431 m in lane 2, moving at a speed of 20 m·s^{-1}, and the leader vehicle (2) is positioned at 491 m in lane 1, moving at a speed of 20 m·s^{-1}.
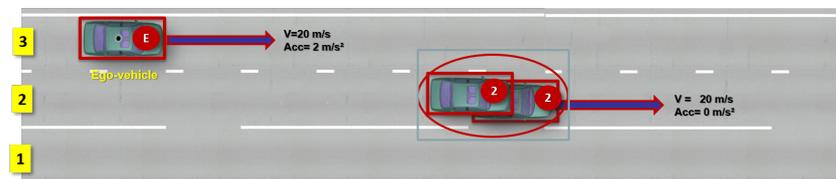

Figure 12. Schematic illustration of scenario 2−E2 with perception uncertainty (scenario B).

To address the perception uncertainty, we employ the Kalman filter [44], which is well-suited for data assimilation to estimate the state and parameter values. We use this filter to predict the vehicle's next position by considering the system and sensor noise. However, we do not incorporate GPS noise in this structure since we calculate it from the data returned by the sensor.

When perception uncertainty exists, as shown in Figure 13, we apply white Gaussian noise to the signal and estimate the position using the Kalman filter. The figure represents an example of the real positioning of a vehicle (green square) and the estimated location (red diamond), obtained by applying the Kalman filter to our application.
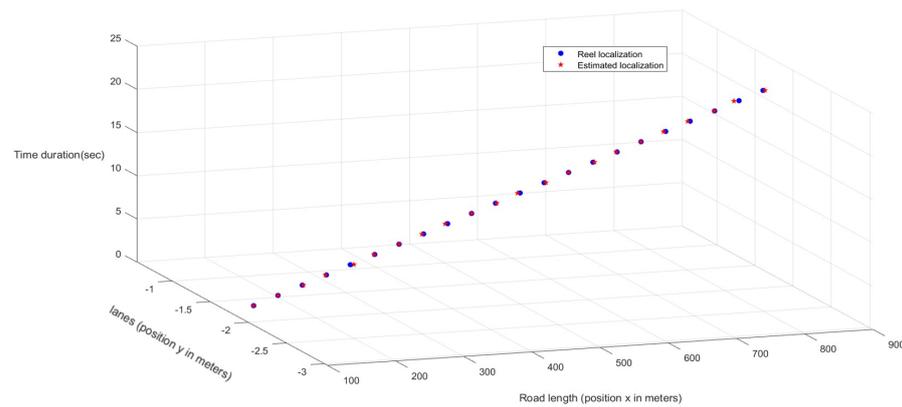
Figure 13. Representation of the real vehicle position superimposed on the estimated location obtained by applying a white Gaussian noise in the Kalman filter method.

For each scenario, we calculated the normalized probability of collision functions of the extended time-to-collision (TTC), extended time-headway (TH), and extended Gruyer distance (DG), as well as the probability of collision associated with them and the probability of the collision indicator based on multi-dimensional modeling and uncertainty (RIMUM). The collision occurs at 9 s.

In scenario 1−E1, both the TTC and TH probability of collisions increase earlier and more rapidly than the RIMUM, making them more effective for anticipation. The increase in the RIMUM probability of collision is closer to the moment of collision. This can be explained by the fact that the TTC and TH probabilities of collision are at their maximum several seconds before the actual collision, while the RIMUM is at its maximum only when the two vehicles collide. In scenario 2−E1, regarding the probability of collision of death, the RIMUM values are low in scenario 1−E2. The probability of collisions based on TTC and TH results in a probability of collision that reaches 0.15, which means a 15% probability of death. This is a high value considering that the vehicles are not on the same lane. RIMUM still displays a high value of 0.07 but is lower than the probability of collision estimators based on TTC and TH. Figure 14 presents extended TH and TTC, the probability of collision based on TH, and the probability of collision based on TTC for scenario 1−E1.
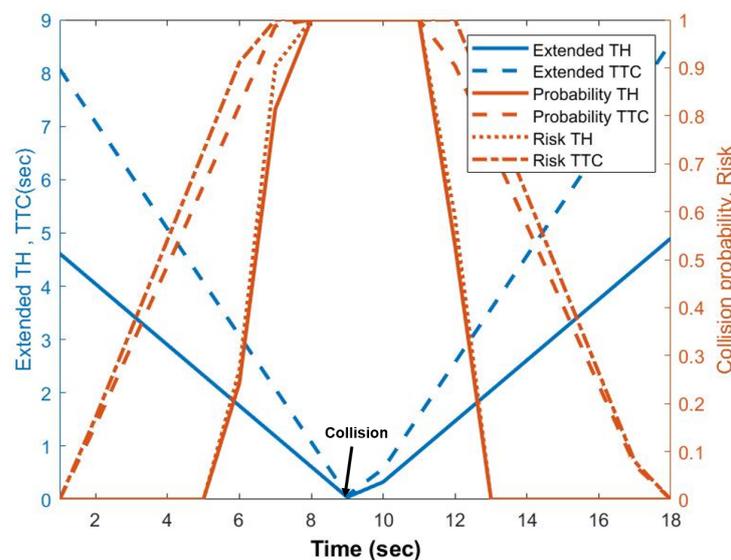

Figure 14. Scenario 1−E1 extended TH and TTC, probability of collision based on TH, probability of collision based on TTC.

5.2. Extended Local Probability of Collision Estimation

To estimate our first extended probability of collision "extended local probability of collision", we used the scenario illustrated in Figure 15. The ego vehicle studied in this situation is in the given branch (B1) of cluster 1, with an average velocity of 12 m·s^{-1}.

The obstacles are the two following leaves (L2 and L3), illustrated by the gray vehicles. Their respective velocities are 34 m·s^{-1} and 26 m·s^{-1}.

The local perception map of the ego-vehicle is obtained using RADAR or light detection and ranging (LiDAR) and the localization uses a GPS.

B1 can only perceive the vehicle in front of it, L1, and cannot see the two leaves, L2 and L3, behind it. This potentially results in two ignored probabilities of collision: R2:{B1,L2} and R3:{B1,L3}, as shown in Figure 15.

However, by using our extended local perception method, we can detect two new vehicles and, thus, estimate two extended local probabilities of collision: R2{B1,L2} and R3{B1,L3}. The likelihood of a collision between vehicles B1 and L2 was assessed using the extended TTC model (depicted in Figure 16) and the TH model (illustrated in Figure 17). The probability of collision between the branch, B1, and the leaf, L2, R2 {B1,L2}, is represented in Figures 18 and 19.
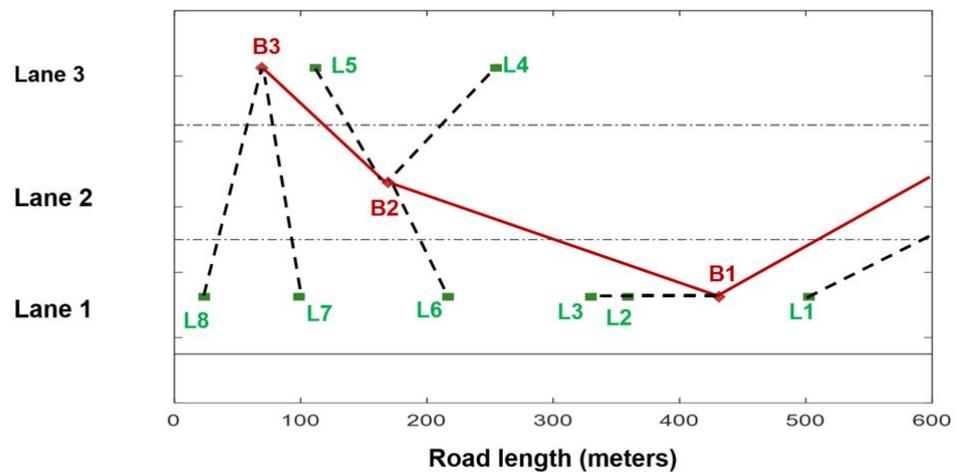

Figure 15. The extended local probability of collision estimation environment (B1).

In this scenario, the extended TTC (Figure 16) and TH (Figure 17) models were used to evaluate the probability of collision between vehicles B1 and L2.

The extended TH model reached its maximum collision probability value one second before the actual collision, while the extended TTC model gave an alert five seconds before the collision, providing a longer reaction time but saturating the probability of collision several seconds before the collision.

The probability of collision for R3 started to increase as the vehicles approached each other, while for R1, the probability of collision decreased as the vehicles moved away from each other. This extended local probability of collision estimation method can provide more accurate and detailed information on the potential collision probability of collisions in complex traffic situations (Figure 18).
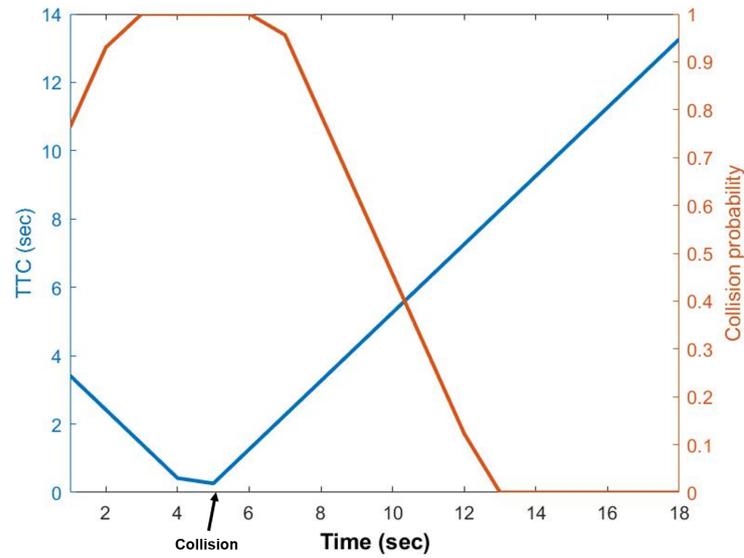
Figure 16. Extended local probability of collision of R2{B1,L2} and collision probabilities for the CBL scenario (A) based on TTC.
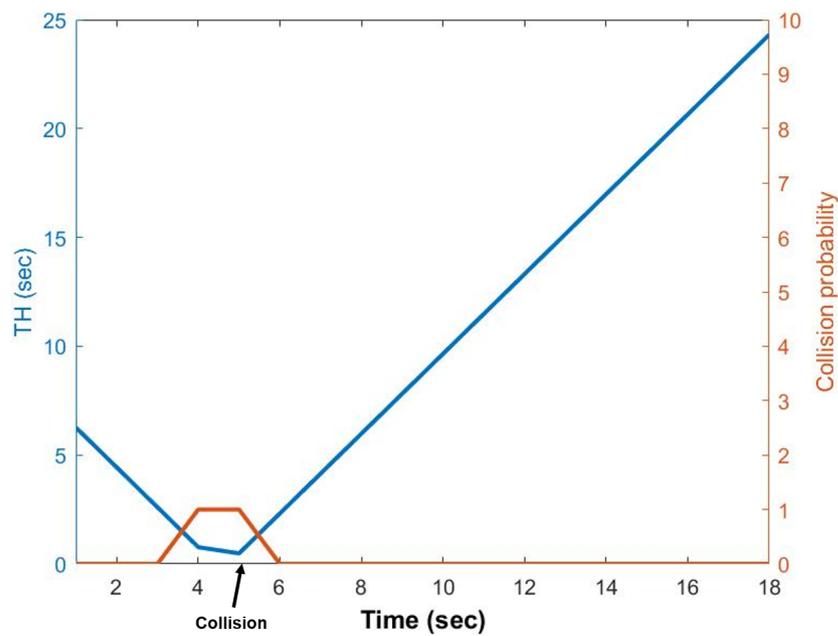

Figure 17. Extended local probability of collision of R2{B1,L2} and collision probabilities for the CBL scenario (A) based on TH.

The probability of collision for R3 started at zero at the beginning of the simulation and increased as the vehicles approached each other, while for R1, the probability of collision started at 0.18 at the beginning of the simulation and decreased as the vehicles moved away from each other.

R2 had the highest probability of collision of all, and we were able to estimate the danger of this second probability of collision five seconds before the collision. The results of scenario B were very close to those of scenario A (the difference was within a hundredth).
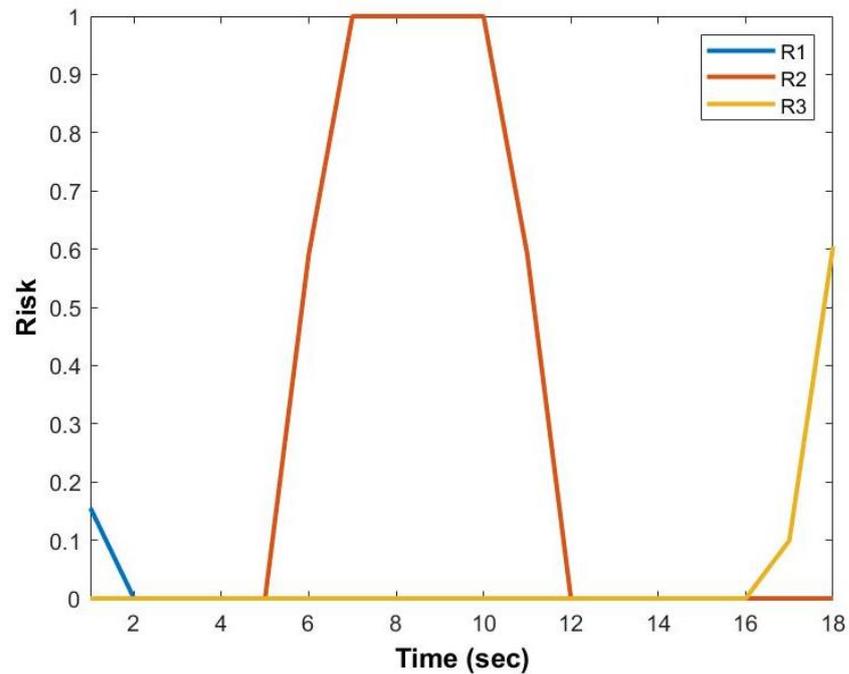
Figure 18. The extended local probability of collision (R1,R2,R3) of B1 in the CBL-G scenario A.
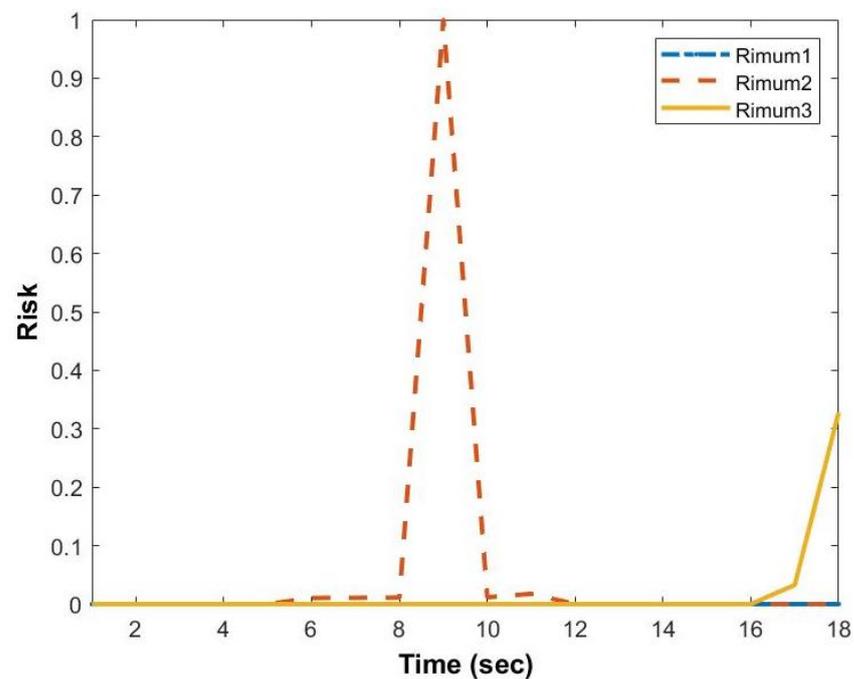

Figure 19. The extended local probability of collision RIMUM (R1,R2,R3) of B1 in the CBL-G scenario A.

The distance between Gruyer and RIMUM reached 1 at the exact moment of the collision. In this situation, RIMUM is more realistic than the estimators based on TTC and TH. However, the estimators based on TTC and TH are more effective in terms of anticipation.

The global probability of collision (GR) of the cluster is the maximum probability of collision that the branch has with its leaves and the maximum probability of collision the branch has with its upstream and downstream branches.

GR = Max{RL,RB} with RL = Max{R{B,i}..., R{B,n}} being the maximum branch-to-leaf probability of collision, with n being the number of leaves in the cluster.

RB = Max$\{R\{B, B_{upstream}\}, R\{B, B_{downstream}\}\}$ being the maximum branch-to-branch probability of collision.

The extension of the local probability of collision estimation allowed us to achieve two main objectives. Firstly, it enabled us to raise the perception of the branch to a level that allowed for the detection of all leaves in the cluster without being constrained by the perception of the onboard equipment. This means that the branch's extended local perception took into account 100% of the average number of leaves per cluster.

Secondly, it allowed us to calculate all potential probabilities of collision ahead of time and provide enough time for the driver or the system to react. As demonstrated, although B1 had a unique local probability of collision R1B1, L1, we were able to estimate two new extended local probabilities of collision, R2B1, L2 and R3B1, L3, using this method. The second probability of collision, R2, was found to be the highest probability of collision of all, and we were able to estimate the danger of the second probability of collision 5 seconds before the collision.

The results of scenario B were very close to those of scenario A (the difference being at the hundredth place).

5.3. Extended Branch Probability of Collision Estimation

The extended branch probability of collision is the probability of collision calculated by the branch in the CBL-G structure from the information transmitted by the adjacent branches (upstream and downstream) of the ego vehicle, i.e., their local perception. This implies that for each Branch (B), we will have several probabilities of collision (R): $\{R\{B, B_{Upstream}\}, R\{B, B_{downstream}\}, R\{B, i\},... R\{B, n\}\}$ with i $\in$ [1, n], n being the number of perceived vehicles by the adjacent branches.

The branch, B2, is the branch of cluster 2; its local perception of B2 is empty, while its extended local perception contains the leaves belonging to its cluster (L1,L2,L3,L4).

As for the two adjacent branches of B2 are B1 (the branch of cluster 1) and B3 (the branch of cluster 3), vehicle B1 perceives vehicle L6, while B3 perceives two vehicles: L5 and L3.

All of these vehicles (B1,B3,L3,L5,L6) are outside of B2's perception range. So, for vehicle B2's extended probability of collision branch estimation, it will consider multiple probabilities of collision: R{B2,B1}, R{B2,B3}, R{B2,L3}, R{B2,L5}, and R{B2,L6}.

The extended branch probability of collision scenario is represented in Figure 20. Unlike the other probability of collision, vehicle L3 is a member of the second cluster, B2, so the probability of collision between vehicle B2 and L3, R{B2,L3}, is estimated in the extended local probability of collision of B2.
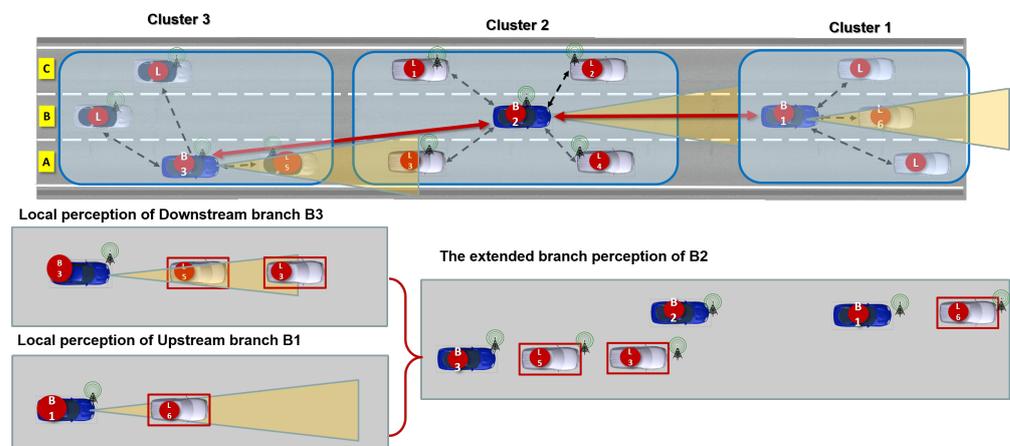

Figure 20. Representation of the extended branch perception of branch B2 in cluster 2 from the extended local perceptions of B1 and B3 for scenario A with correct perception and perfect localization.

The inter-distance between branches B1, B2, and B3 is 500 m. Vehicle B2 is in lane B traveling at a speed of 15 m/s. Vehicle L5 is in lane A moving at 32 m/s. The extended branch probability of collision between B2 and L5 is R5{B2,L5}. R5 results show that the probability of collision is low, with a speed difference of 5 m/s; however, it showed an increase at the 19th second when vehicle L5 overtook vehicle B2. Regarding the probability of collision, RIMUM has a very low value (0.17), which can be explained by the differential speed of 5 m/s, and also considering that the severity function is null; for the extended TTC and TH values, which are low (0.49 and 0.42) but still high considering this driving situation, since the vehicles are in different lanes, RIMUM presents the lowest value and, thus, is the most realistic estimate for this case.

We observe that the perception of the downstream branch is part of the ego branch's local extended perception, which creates redundancy. Indeed, the detected vehicles in the extended branch perception are—most of the time—already present in the local extended perception, which creates a duplication of the probability of collision assessment since this probability of collision is already calculated at the level of the extended probability of collision of the ego branch.

On the other hand, we noticed that the extended branch probability of collision, based on the upstream branch perception, brings a new perception and, thus, allows us to estimate a more distant probability of collision, making it more relevant. Following these results, we will only use the perception of the upstream branch in our future works. Nonetheless, this discovery is not a flaw, but rather a strength of the method. This redundancy can be used to improve the certainty, reliability, and robustness of the probability of collision indicators that utilize it. As a result, a more comprehensive probability of collision estimation will be required.

The extended branch probability of collision estimation method was applied to evaluate the probability of collision between vehicles B1 and L2, which eventually collided at 5 s. The extended TTC and TH values were deemed high but still acceptable given the driving situation. RIMUM was considered the most realistic in this situation, with a very low probability of collision of 0.17, as explained by differential speed and zero gravity function.

The results show that the downstream branch perception creates redundancy as it is often already taken into account in the extended local perception of the ego branch, creating a duplication of the probability of collision assessment. On the other hand, upstream branch perception allowed for estimating a more distant probability of collision, making it more relevant.

5.4. Global Probability of Collision Estimation

This probability of collision is calculated by the branch nodes only, based on the information collected from the communication outside of the clusters i.e., indirect communication between branches that are more than one hop away.

The global probability of collision estimation scenario is described as follows: The ego vehicle is the branch, B3, illustrated in Figure 21. The neighboring branches are B2 and B4. Vehicle B3's perception contains vehicle B4, the perception of the vehicle of the downstream branch, B2, contains vehicles B3 and B4, and the perception of the upstream branch, B4, does not contain any vehicles. In this case, these neighboring branches (one hop) do not give the ego vehicle (B3) the possibility of adding new vehicles to its perception outside its two neighboring branches (up and down).

However, the global probability of collision is based on the extended local perception of the branches beyond one hop; so, to calculate the global probability of collision of the branch (B3), we use the extended local perception of the B1 and B5 branches, i.e., the leaves: L1, L2, and L3.

The global probability of collision between the branch (B3) and the leaf (L1) is the probability of collision R1{B3,L1}, the global probability of collision between the branch (B3) and the leaf (L2) is the probability of collision R2{B3,L2}, and the global probability of

collision between the branch (B3) and the leaf (L3) is the probability of collision R3{B3,L3}. The overall global probability of collision of the branch (B3) is GR = Max{R1,R2,R3}.
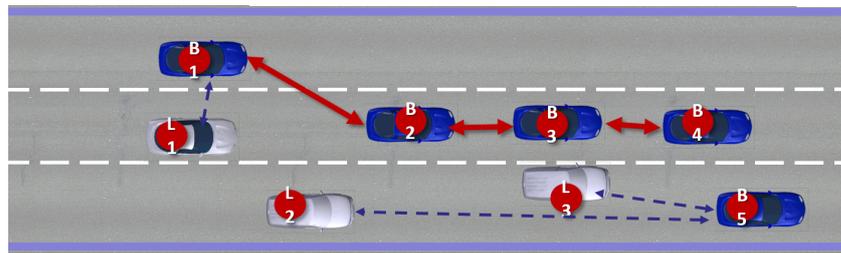

Figure 21. The road section studied in the context of the global probability of collision estimation.

In this scenario, we do not create any probability of collision situations; instead, we estimate the overall probability of collision. B3 travels in the second lane at an average speed of 35 m/s, while L2 travels in the third lane at about 26 m/s.

The vehicle (L3) travels in the third lane at a speed of 29 m per second. This means that the L3 vehicle and the ego vehicle are nearby and parallel. In a longitudinal position, the two vehicles are less than 4 m apart at the moment (6 s). This type of scenario can be considered similar to scenario1-E2 studied for the estimation of the local probability of collision.

Vehicle L1 drives in the same lane and behind vehicle B3 at a speed close to the B3 branch speed (35 m/s). At the start of the simulation, the distance between B3 and L1 is 100 m, so the R1 probability of collision should be very low. To simulate a probability of collision situation, we adapt the speed of the rear vehicle, i.e., we assume that the driver accelerates until reaching a speed of 45 m/s; the collision happens at 14 s.

By using the global probability of collision, we estimated a collision probability 7 s before the actual collision. Indeed, the local probability of collision of B3 allows us to estimate only one close probability of collision (with B4); however, the global probability of collision allows us to estimate many new distant probabilities of collision (R1, R2, R3), as represented in Figure 22. By their definitions, the probability of collision is physically distant for the most part and the level of the probability of collision remains low. However, in terms of anticipation, it proves to be effective. Indeed, if we task the RSU or another element with launching an alert system with a threshold of 0.6, for example, we will be able to detect the vehicle 14 seconds ahead and anticipate the collision probability by 7 s.
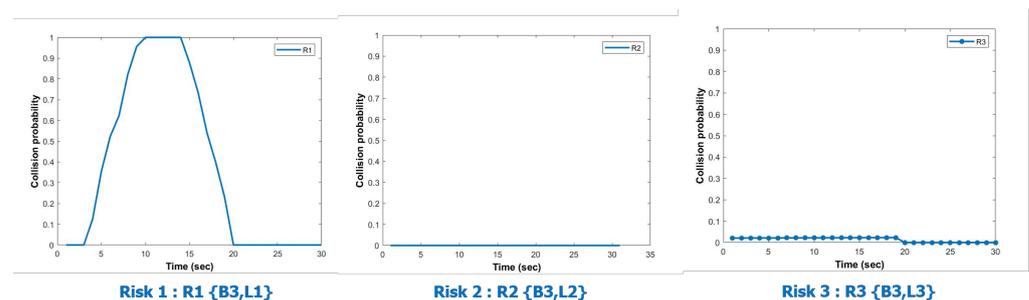

Risk 1 : R1 {B3,L1} **Risk 2 : R2 {B3,L2}** **Risk 3 : R3 {B3,L3}**

Figure 22. Representation of collision probability of collision R3{B3,L3}.

The global probability of collision is based on the extended local perception of branches beyond a hop and is calculated by the branch for each leaf. To estimate the global probability of collision of branch B3, we use the extended local perception of branches B1 and B5, allowing us to calculate a more distant probability of collision with leaves L1, L2, and L3. Using the concept of the global probability of collision, we were able to predict a collision probability of collision 7 seconds before it occurred.

The global probability of collision allowed for detecting three new distant probabilities of collision (R1, R2, R3). Although these probabilities of collision are physically distant and

have a low level of probability of collision, their anticipation proves to be effective in terms of safety. Thus, if we program the RSU or any other element to trigger an alert system with a threshold of 0.6, for example, we can detect the presence of the vehicle 14 s in advance and anticipate a collision probability of collision of 7 s.

Regarding the probability of collision metrics, the results suggest that the RIMUM is a useful tool for modeling the probability of collisions associated with different vehicle configurations. It takes into account the multi-dimensional nature of the problem and the uncertainty associated with it, providing a more accurate representation of the probability of collisions involved. The study also highlights the importance of considering different scenarios and situations when modeling the probability of collisions associated with vehicle configurations.

6. Conclusions and Perspectives

In this paper, we presented a comprehensive approach to the probability of collision estimation in intelligent transportation systems, specifically addressing connected and autonomous vehicles. Our study covered various aspects, including the evaluation of the probability of collision methods, vehicle modeling with uncertainties, and multi-dimensional configurations between vehicles, leading to multi-level collision probability estimations.

In our exploration of collision probability evaluation methods, we carefully selected metrics such as time-to-collision (TTC), modified time-to-collision (MTTC), time-integrated time-to-collision (TIT), as well as alternative approaches like time-to-closest-encounter (TTCE), and responsibility-sensitive safety (RSS). These metrics were chosen based on their widespread use and recognition in the literature, making them suitable for comparative analysis and providing a comprehensive understanding of collision probability.

Our proposal included a detailed representation of vehicle configurations using rectangles and ellipsoids, and we introduced the concept of the Gruyer distance for multi-dimensional modeling. These choices were motivated by their practical relevance in capturing the dynamic nature of real-world driving scenarios, enhancing the realism of our collision probability estimation framework.

Regarding the spatial arrangement of cars and the consideration of speed modes and the number of lanes, our choices were informed by their significance in influencing collision probabilities. However, it is essential to acknowledge that our simulations might not encompass all possible real-world scenarios, and certain limitations exist in the representatives of the chosen configurations. We aimed to simulate scenarios that are not only common but also critical in determining collision probability. While there may be various options, the chosen configurations were deemed representative and impacted in evaluating the effectiveness of our proposed methodology.

In summary, our choices in metrics, vehicle modeling, and spatial configurations were carefully considered to ensure the relevance and practical applicability of our collision probability estimation framework. We believe that these choices contribute to the robustness and effectiveness of our proposed methodology in enhancing road safety in the era of connected and autonomous vehicles.

Looking forward, future research could further explore alternative configurations and assess their impact on collision probability, providing additional insights into the complexities of intelligent transportation systems.

References

1. Wang, J.; Liu, J.; Kato, N. Networking and Communications in Autonomous Driving: A Survey. *IEEE Commun. Surv. Tutor.* **2019**, *21*, 1243–1274. [CrossRef]
2. Aydogan, D.; Tatkeu, C.; Hillali, Y.E. Pilot Based Stepped-Carrier OFDM to Retrieve High Resolution Range-Velocity Profile in Joint Vehicular Communication and Radar Systems. In Proceedings of the 2022 International Conference on Communications, Information, Electronic and Energy Systems (CIEES), Veliko Tarnovo, Bulgaria, 24–26 November 2022; pp. 1–6. [CrossRef]
3. Sharma, S.; Nidhi. Vehicular Ad-Hoc Network: An Overview. In Proceedings of the 2019 International Conference on Computing, Communication, and Intelligent Systems (ICCCIS), Greater Noida, India, 18–19 October 2019; pp. 131–134. [CrossRef]
4. Ayyub, M.; Oracevic, A.; Hussain, R.; Khan, A.A.; Zhang, Z. A Comprehensive Survey on Clustering in Vehicular Networks: Current Solutions and Future Challenges. *Ad Hoc Netw.* **2022**, *124*, 102729. [CrossRef]
5. Senouci, O.; Zibouda, A.; Harous, S. Survey: Routing protocols in vehicular ad hoc networks. In Proceedings of the 2nd International Conference on Advanced Wireless Information, Data, and Communication Technologies, Paris, France, 13–14 November 2017; Hamdan, H., Ed.; ACM International Conference Proceeding Series; Association for Computing Machinery: Melbourne, Australia, 2017. [CrossRef]
6. Lu, Z.; Qu, G.; Liu, Z. A Survey on Recent Advances in Vehicular Network Security, Trust, and Privacy. *IEEE Trans. Intell. Transp. Syst.* **2019**, *20*, 760–776. [CrossRef]
7. Boyinbode, O.; Le, H.; Mbogho, A.; Takizawa, M.; Poliah, R. A Survey on Clustering Algorithms for Wireless Sensor Networks. In Proceedings of the International Conference on Network-Based Information Systems (NBIS), Takayama, Japan, 14–16 September 2010; pp. 358–364. [CrossRef]
8. Liu, X. A Survey on Clustering Routing Protocols in Wireless Sensor Networks. *Sensors* **2012**, *12*, 11113–11153. [CrossRef] [PubMed]
9. Dua, A.; Kumar, N.; Bawa, S. A systematic review on routing protocols for Vehicular Ad Hoc Networks. *Veh. Commun.* **2014**, *1*, 33–52. [CrossRef]
10. Cooper, C.; Franklin, D.; Ros, M.; Safaei, F.; Abolhasan, M. A Comparative Survey of VANET Clustering Techniques. *IEEE Commun. Surv. Tutor.* **2016**, *19*, 657–681. [CrossRef]
11. Ramakrishnan, B.; Professor, A.; Rajesh, R.; Shaji, R.; Professor, A. CBVANET: A Cluster Based Vehicular Adhoc Network Model for Simple Highway Communication. *Int. J. Adv. Netw. Appl.* **2011**, *755*, 2–4.
12. Guizani, B. Clustering Algorithms and Routing Protocaols in Wireless Mobile Networks. Ph.D. Thesis, Université de Technologie de Belfort-Montbeliard, Belfort, France; Université de la Manouba, Tunisie, Tunisia, 2012.
13. Sathya Narayanan, P.; Joice, C.S. Vehicle-to-Vehicle (V2V) Communication using Routing Protocols: A Review. In Proceedings of the 2019 International Conference on Smart Structures and Systems (ICSSS), Chennai, India, 14–15 March 2019; pp. 1–10. [CrossRef]
14. Husnain, G.; Anwar, S.; Sikander, G.; Ali, A.; Lim, S. A Bio-Inspired Cluster Optimization Schema for Efficient Routing in Vehicular Ad Hoc Networks (VANETs). *Energies* **2023**, *16*, 1456. [CrossRef]
15. Shan, M.; Narula, K.; Wong, Y.F.; Worrall, S.; Khan, M.; Alexander, P.; Nebot, E. Demonstrations of Cooperative Perception: Safety and Robustness in Connected and Automated Vehicle Operations. *Sensors* **2021**, *21*, 200. [CrossRef]
16. Rahman, M.S.; Abdel-Aty, M.; Wang, L.; Lee, J. Understanding the Highway Safety Benefits of Different Approaches of Connected Vehicles in Reduced Visibility Conditions. *Transp. Res. Rec.* **2018**, *2672*, 91–101. [CrossRef]
17. ETSI. Analysis of the Collective Perception Service (CPS). Technical Report, Version TR 103 562—V2.1.1. 2019. Available online: https://www.google.com/url?sa=t&rct=j&q=&esrc=s&source=web&cd=&cad=rja&uact=8&ved=2ahUKEwiQpJz2 vMGDAxVRVqQEHSQFDG0QFnoECA4QAQ&url=https%3A%2F%2Fwww.etsi.org%2Fdeliver%2Fetsi_tr%2F103500_103599 %2F103562%2F02.01.01_60%2Ftr_103562v020101p.pdf&usg=AOvVaw17GdcoGqBrBUuLLxaU0NJ-&opi=89978449 (accessed on 11 December 2023).
18. Martin, F.; Tarek, S. Safety Evaluation of Connected Vehicles for a Cumulative Travel Time Adaptive Signal Control Microsimulation Using the Surrogate Safety Assessment Model. In Proceedings of the Transportation Research Board 96th Annual Meeting, Washington, DC, USA, 8–12 January 2017.
19. Olia, A.; Abdelgawad, H.; Abdulhai, B.; Razavi, S.N. Assessing the Potential Impacts of Connected Vehicles: Mobility, Environmental, and Safety Perspectives. *J. Intell. Transp. Syst.* **2016**, *20*, 229–243. [CrossRef]
20. Paikari, E.; Tahmasseby, S.; Far, B. A simulation-based benefit analysis of deploying connected vehicles using dedicated short range communication. In Proceedings of the 2014 IEEE Intelligent Vehicles Symposium Proceedings, Dearborn, MI, USA, 8–11 June 2014; pp. 980–985. [CrossRef]
21. Karbasi, A.; O'Hern, S. Investigating the Impact of Connected and Automated Vehicles on Signalized and Unsignalized Intersections Safety in Mixed Traffic. *Future Transp.* **2022**, *2*, 24–40. [CrossRef]
22. Freitas, J.D.; Censi, A.; Smith, B.W.; Lillo, L.D.; Anthony, S.E.; Frazzoli, E. From driverless dilemmas to more practical commonsense tests for automated vehicles. *Proc. Natl. Acad. Sci. USA* **2021**, *118*, e2010202118. [CrossRef] [PubMed]
23. Fayyad, J.; Jaradat, M.A.; Gruyer, D.; Najjaran, H. Deep Learning Sensor Fusion for Autonomous Vehicle Perception and Localization: A Review. *Sensors* **2020**, *20*, 4220. [CrossRef] [PubMed]
24. Tian, D.; Zhou, J.; Wang, Y.; Sheng, Z.; Xia, H.; Yi, Z. Modeling chain collisions in vehicular networks with variable penetration rates. *Transp. Res. Part Emerg. Technol.* **2016**, *69*, 36–59. [CrossRef]

25. Belmekki, S.; Gruyer, D.; Tatkeu, C. Chain Branch Leaf-Gateway, a Strategy for Dynamic Clustering and Optimal Coverage of Communication for Automated Mobility. In Proceedings of the 2022 IEEE 2nd International Conference on Digital Twins and Parallel Intelligence (DTPI), Boston, MA, USA, 24–28 October 2022; pp. 1–5. [CrossRef]

26. Belmekki, S. Multi-Level Risk and Collective Perception for High Quality of Service Automated Mobility in a Highly Dynamic V2X Connected Environment. Ph.D. Thesis, Université de Lille, Lille, France, 2023.

27. Belmekki, S.; Tatkeu, C.; Gruyer, D. Performance Evaluation of Routing Protocols in Vehicular Ad Hoc Networks. In Proceedings of the 18th International Conference for Internet Technology and Secured Transactions (ICITST-2023), Oxford, UK, 13–15 November 2023.

28. Thandavarayan, G.; Sepulcre, M.; Gozalvez, J. Generation of Cooperative Perception Messages for Connected and Automated Vehicles. *IEEE Trans. Veh. Technol.* **2020**, *69*, 16336–16341. [CrossRef]

29. Mattas, K.; Makridis, M.; Botzoris, G.; Kriston, A.; Minarini, F.; Papadopoulos, B.; Re, F.; Rognelund, G.; Ciuffo, B. Fuzzy Surrogate Safety Metrics for real-time assessment of rear-end collision risk. A study based on empirical observations. *Accid. Anal. Prev.* **2020**, *148*, 105794. [CrossRef]

30. Charly, A.; Mathew, T.V. Estimation of traffic conflicts using precise lateral position and width of vehicles for safety assessment. *Accid. Anal. Prev.* **2019**, *132*, 105264. [CrossRef]

31. Demmel, S. Construction of Extended Maps of Road Difficulties Based on the Fusion of Local Maps. Ph.D. Thesis, University of Versailles, French Institute of Science and Technology of Transport, Development Networks, Versailles, France, 2013.

32. Eggert, J.; Puphal, T. Continuous Risk Measures for ADAS and AD. 2017. Available online: https://www.honda-ri.de/pubs/pdf/3507.pdf (accessed on 11 December 2023).

33. Shi, X.; Wong, Y.; Li, M.; Chai, C. Key risk indicators for accident assessment conditioned on pre-crash vehicle trajectory. *Accid. Anal. Prev.* **2018**, *117*, 346–356. [CrossRef]

34. Johnsson, C.; Laureshyn, A.; Ceunynck, T.D. In search of surrogate safety indicators for vulnerable road users: A review of surrogate safety indicators. *Transp. Rev.* **2018**, *38*, 765–785. [CrossRef]

35. Tarko, A.P. Surrogate measures of safety. In *Safe Mobility: Challenges, Methodology and Solutions*; Emerald Publishing Limited: Bingley, UK, 2018.

36. Mobileye, I. RSS: Responsibility-Sensitive Safety for Autonomous Vehicles. *arXiv* **2018**, arXiv:1802.01781.

37. Chai, C.; Zeng, X.; Wu, X.; Wang, X. Safety Evaluation of Responsibility-Sensitive Safety (RSS) on Autonomous Car-Following Maneuvers Based on Surrogate Safety Measurements. In Proceedings of the 2019 IEEE Intelligent Transportation Systems Conference (ITSC), Auckland, New Zealand, 27–30 October 2019; pp. 175–180. [CrossRef]

38. Koopman, P.; Osyk, B.; Weast, J. Autonomous Vehicles Meet the Physical World: RSS, Variability, Uncertainty, and Proving Safety. In *Computer Safety, Reliability, and Security*; Romanovsky, A., Troubitsyna, E., Bitsch, F., Eds.; Springer: Cham, Switzerland, 2019; pp. 245–253.

39. Fox, C.; Camara, F.; Markkula, G.; Romano, R.; Madigan, R.; Merat, N. *When Should the Chicken Cross the Road?—Game Theory for Autonomous Vehicle—Human Interactions*; Science and Technology Publications, Lda: Setúbal, Portugal, 2018.

40. Muzahid, A.J.M.; Kamarulzaman, S.F.; Rahman, M.A.; Murad, S.A.; Kamal, M.A.S.; Alenezi, A.H. Multiple vehicle cooperation and collision avoidance in automated vehicles: Survey and an AI-enabled conceptual framework. *Sci. Rep.* **2023**, *13*, 603. [CrossRef] [PubMed]

41. Leroy, J.; Gruyer, D.; Orfila, O.; El Faouzi, N.E. Adapted Risk Indicator For Autonomous Driving System with Uncertainties and Multi-Dimensional Configurations Modeling. In Proceedings of the 2021 IEEE International Intelligent Transportation Systems Conference (ITSC), Indianapolis, IN, USA, 19–22 September 2021; pp. 2034–2041. [CrossRef]

42. Mahajan, V.; Katrakazas, C.; Antoniou, C. Prediction of Lane-Changing Maneuvers with Automatic Labeling and Deep Learning. *Transp. Res. Rec.* **2020**, *2674*, 336–347. [CrossRef]

43. Demmel, S.; Gruyer, D.; Rakotonirainy, A. Comparing cooperative and non-cooperative crash risk-assessment. In Proceedings of the 2013 IEEE Intelligent Vehicles Symposium (IV), Gold Coast, Australia, 23–26 June 2013; pp. 1007–1013. [CrossRef]

44. Iglesias, M.A.; Law, K.J.; Stuart, A.M. Ensemble Kalman methods for inverse problems. *Inverse Probl.* **2013**, *29*, 045001. [CrossRef]